

LCF behavior and microstructure of alpha-brass CuZn30 under uniaxial, planar-biaxial and tension-torsion loading conditions

S. Henkel¹, A. Weidner¹, H. Biermann¹, H.-J. Kühn², B. Rehmer², N. Sonntag¹

¹ Institute of Materials Engineering, Technische Universität Bergakademie Freiberg, Gustav-Zeuner-Straße 5, 09599 Freiberg, Germany, henkel@ww.tu-freiberg.de

² BAM Federal Institute for Materials Research and Testing, Unter den Eichen 87, 12205 Berlin, Germany, birgit.rehmer@bam.de

ABSTRACT. *The low-cycle fatigue behavior of α -brass CuZn30 was investigated in uniaxial (tension-compression and torsional) and biaxial tests under total strain control at room temperature. Planar-biaxial fatigue tests were carried out on a servohydraulic tension-compression testing machine with and without phase shift using a cruciform specimen geometry with fixed principal stress axes. In phase and out of phase tension-torsion tests were performed using tube shape specimens on a servohydraulic tension-torsion testing machine. Microstructural investigations were performed by transmission electron microscopy as well as by scanning electron microscope. For all proportional load cases the equivalent strain amplitude based on a maximum shear strain energy criterion results in a similar hardening behavior and in fatigue life times within a scatter band of three. Out of phase loading results in additional cyclic hardening and reduced life time. Planar glide structures were observed in all tested cases as well as areas of pronounced strain localization in the torsional load cases. No evidence of transition to wavy glide behavior was observed.*

INTRODUCTION

In the literature only few studies on the microstructure evolution under multiaxial loading are available. In the past, especially stainless steels but also copper as a model material for wavy glide behavior were investigated. Doong et al. [1] studied the microstructure development of stainless steel grades 304 and 310 (showing mainly planar glide) as well as aluminium and copper (showing wavy glide) under tension-torsion loading with rotating principal stress axes. They found for the non proportional case that planar slip materials exhibit multi slip structures and extra hardening due to the activation of several slip systems.

Zhang and Jiang [2] studied on polycrystalline copper the influence of texture under tension-torsion loading conditions. Under non-proportional loading with time varying principal stress directions, the influence of the texture on the stress-strain behavior was not significant, but more slip systems were activated compared to proportional loading.

The resultant saturation stress was inversely proportional to the dislocation cell size. The relationship between stress and strain amplitude was almost completely reversible: After the change from a higher to lower strain amplitude or from a load with a rotating axes system to proportional loading the original stress level was resumed. This means basically that the material behavior is largely independent from the load history, while there was also shown that the dislocation arrangements were not completely reversible. For the austenitic steel 800H under proportional LCF loading dislocation cell structures were observed while under nonproportional tension-torsion load disordered dislocation structures with higher dislocation densities were found [3]. Due to a strong additional strengthening a significant reduction in life time from 2500 cycles to 15-30 cycles was observed. The present work is intended to give a contribution on microstructural understanding of biaxial fatigue on planar glide material.

MATERIAL AND METHODS

For the present investigation the single phase α -brass alloy CuZn30 (69.2% copper and 30.7% zinc) was chosen as a model material. CuZn30 has a very low stacking fault energy and exhibits a high degree of short range order in the microstructure [4]. The material was supplied as hot rolled plates with a thickness of app. 15 mm from Wieland-Werke AG, Germany. The mechanical properties from tensile tests according to DIN EN 10002, the elastic constants measured with impulse echo method and the grain size determined by linear intercepts of grain boundaries according to DIN EN ISO 643 are given in table 1.

The biaxial LCF deformation experiments were conducted strain controlled on tube shape specimens under tension-torsion conditions according to ASTM E 2207. For that purpose a servohydraulic testing system from MTS equipped with two load cells, 50 kN and 500 Nm, was used (Figure 1a). The specimens had a gauge length of 30 mm with a diameter of 13 mm and a wall thickness of 1.5 mm. That means that the requirements of ASTM E 2207 for the wall thickness / diameter ratio of 1:10 were not fulfilled. The inner surface was finished by honing. The outer surface of the specimens was mechanically polished until 6 μm roughness. In phase (IP) and out of phase (OP) loading cycles were applied with a constant frequency of 0.15 Hz. Figure 2 shows the different loading relations between tension and torsion loading: (i) proportional loading (triangular shape), (ii) out of phase loading (90° phase shift sine shape) with circle path, (iii) out of phase loading with box path (alternating ramps in tension and torsion). The planar biaxial tests were performed on a 250 kN servohydraulic test rig (Figure 1b) using cruciform specimens with a thinned central area of diameter 15 mm and 1.6 mm thickness. The specimens were milled and polished mechanically. Total strain controlled ramp load was applied with a frequency of 0.3 Hz using a biaxial orthogonal extensometer. The amplitude in both loading axes was equal while the phase between the loading axes was varied as 0°, 22.5°, 45° and 90°. The stress response was calculated from global elastic synchronous unloading according to [5]. Uniaxial LCF tests were done for comparison in tension-compression on a 100 kN servohydraulic

testing system using conventional LCF specimen bars and under pure torsion on the tension-torsion system using tubular specimens.

After mechanical tests, specimens were cut out of the tubular specimens perpendicular to the tension-compression axis for microstructural investigations. For TEM studies thin foils were prepared by electrolytically thinning. The preparation of specimens for SEM investigations ends up with a vibration polishing procedure. The TEM investigations were done on a Jeol 4000 FX with 400 kV acceleration voltage. Electron channelling contrast imaging (ECCI) technique was applied in a high resolution field emission SEM MIRA3 XMU from TESCAN Company.

Table 1. Mechanical properties of the investigated α -brass alloy CuZn30 (UTS – ultimate tensile strength, YS – yield strength, A₅ – elongation to rupture)

UTS [MPa]	YS [MPa]	A ₅ [%]	Young's modulus [GPa]	Poisson ratio	Grain Size [μm]
339	113	65	110	0.345	33

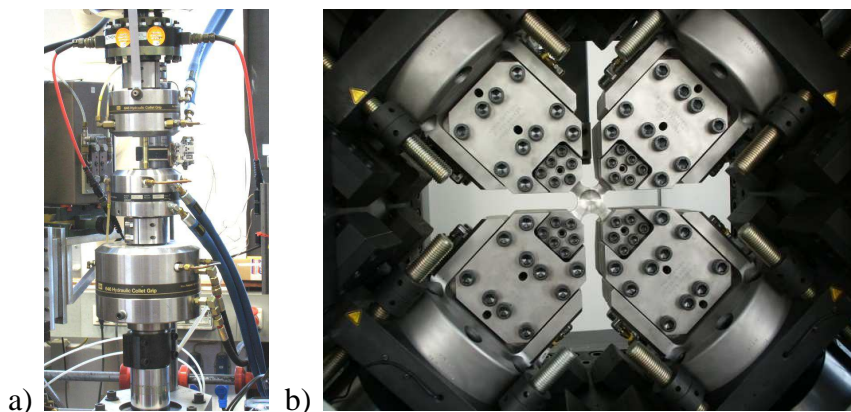


Figure 1: a) Tension-torsion test device with tubular specimen at BAM Berlin, b) planar-biaxial test system with cruciform LCF specimen at TU Bergakademie Freiberg.

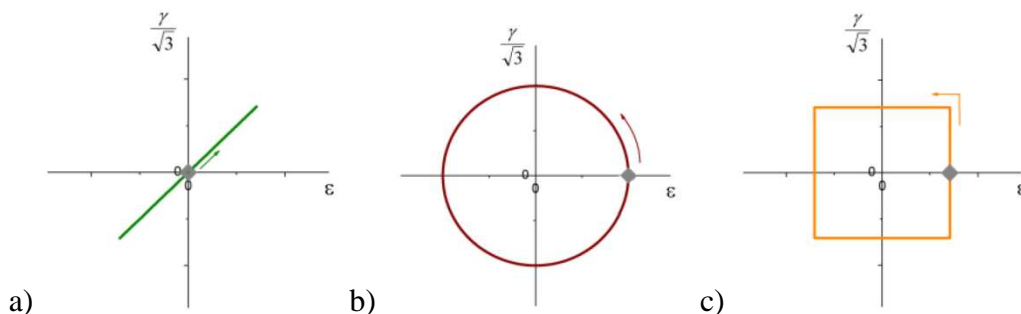


Figure 2: Tension torsion load cases in the ϵ - $\gamma/\sqrt{3}$ -plane: a) proportional, b) non proportional circular (90° phase shifted sine) and c) non proportional box path (alternating ramp load).

RESULTS AND DISCUSSION

Figures 3 and 4 show the cyclic deformation curves for tests with approximately 0.5 % and 1 % equivalent strain amplitude. The maximum equivalent stress amplitude (von Mises) is plotted versus the number of cycles N . For all load cases initial cyclic hardening was observed followed by cyclic softening or cyclic saturation. In addition, a secondary hardening occurred under uniaxial and planar biaxial loading conditions. In the planar-biaxial cases, both axes were deformed with total strains of 0.28 % (resulting in 0.49 % equivalent strain amplitude in the synchronous case) and 0.53 % (resulting in 0.97 % equivalent strain amplitude in the synchronous case), respectively. The phase shifted planar biaxial loads result in lower equivalent strain amplitudes at fixed total strain amplitudes in the two loading axes. The equivalent strain amplitude shows a small variation during the test due to cyclic hardening and consequently changes in the effective Poisson ratio. The given values for the cyclic strain amplitudes in the legend are therefore determined at half lifetime.

The OP tension-torsion tests with circle and box loading path show a pronounced initial hardening within the first few cycles. For both amplitudes the circle path results in the strongest hardening. Shamsaei and Fatemi [6] suggested an approximation of the additional hardening formulated as the non proportional parameter α_{np} (which is defined as the quotient of the stress amplitudes in OP loading and IP loading minus one) from the uniaxial Ramberg-Osgood constants for the monotonic and cyclic stress strain curves which are given for the present material in table 2. The calculated and measured values of α_{np} from the circle path at maximum stress are also given in this table. It can be shown that the correlation gives a good conservative prediction. For the strain amplitude of 1% the measured value is much lower than the calculated value. It can be understood taking into account that the reason for the measured cyclic softening is mainly micro crack formation and propagation and not a real cyclic softening of the bulk material.

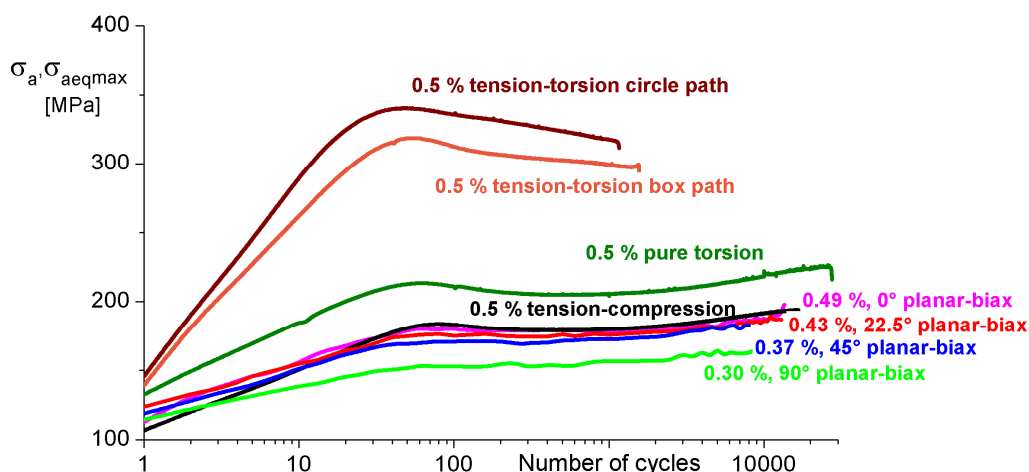


Figure 3: Cyclic deformation curves for uniaxial as well as biaxial tension-torsion and planar-biaxial tests with small equivalent strain amplitudes.

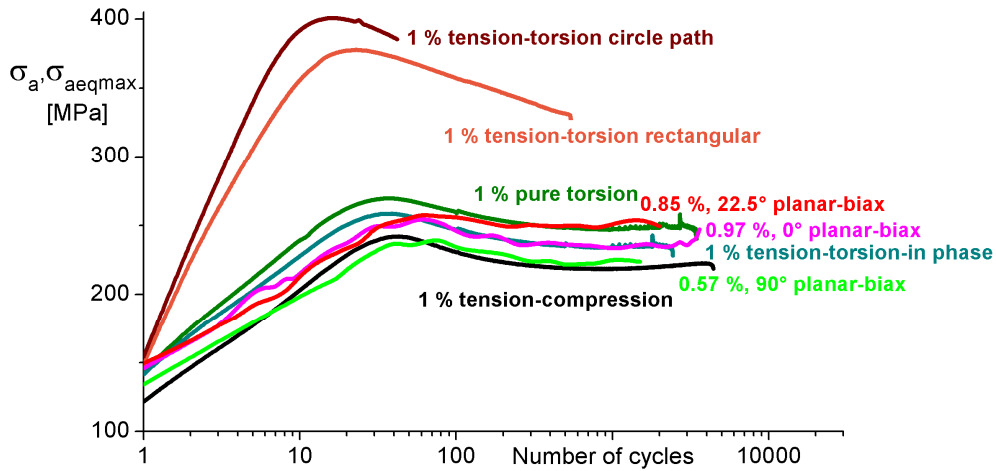


Figure 4: Cyclic deformation curves for uniaxial as well as biaxial tension-torsion and planar-biaxial tests with large equivalent strain amplitudes.

Table 2: Ramberg-Osgood parameters for monotonic (n , K) and cyclic (n' , K') stress strain curves, calculated (α_{np}^c) and measured (α_{np}^m) non proportional factors.

n	K	n'	K'	α_{np}^c (0.5%)	α_{np}^m (0.5%)	α_{np}^c (1%)	α_{np}^m (1%)
0.153	191	0.258	633	0.69	0.60	0.73	(0.55)

The resulting fatigue life time diagram is given in Figure 5. For all proportional cases (tension-compression, torsion, planar-biaxial synchronous, tension-torsion in phase) the life times are within a scatter band of factor three. The fatigue life times of the phase shifted biaxial tests are significantly lower. For an equivalent strain amplitude of 1% the fatigue life time is reduced from app. 4000 cycles to 45 cycles in the tension-torsion circle path. This loading path results in chronologically rotating principle stress axes during cycling and thereby avoid reversible plastic deformation on the slip systems which results also in the strong initial hardening. In contrast in all planar-biaxial load cases there are fixed principal stress axes in the center of the cruciform specimen. The crack starts always in the junction between the measurement area and the smooth radius to the thicker part of the specimen. It is assumed that in these slightly notched areas also rotating principal stress axes occur under phase shifted loads. The non proportional tension-torsion loads result in the lowest fatigue lives. The circle path gives a stronger life time reduction than the box path.

Both the SEM and TEM investigations revealed a pronounced planar glide behavior in all deformation states. No evidence for a transition to wavy glide behavior was found. Figures 6 and 7 show TEM images for an equivalent total strain amplitude of 0,5 % for pure torsion and for out of phase tension-torsion load with circle path at half lifetime, respectively. The bands of dislocation rich areas in Figure 6a) are so-called persistent lüders bands (PLB) [7], which are not so active like persistent slip bands (PSB) in wavy glide materials. Therefore, some authors call them also intense slip bands (ISB) [8].

Such arrangements are found in uniaxial tension-compression, synchronous planar-biaxial and torsion specimens. Especially after torsion and tension-torsion loading, additional strong slip localisation areas were found, which are most probable micro twins (Figure 7). Figure 8 shows the same microstructural feature obtained by electron channelling contrast imaging in the SEM on a specimen deformed at an equivalent strain amplitude of 1 % until final fracture. Persistent lüders bands were not found in all investigated OP tension-torsion specimens at fracture and half lifetime.

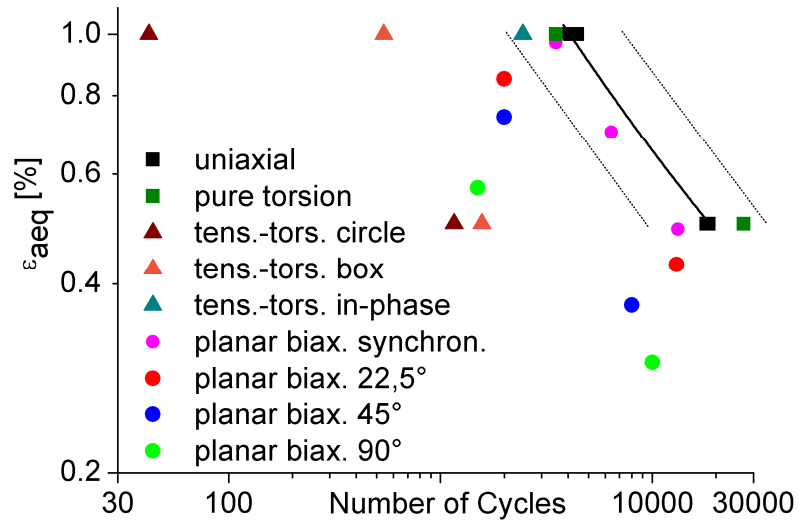


Figure 5: Fatigue live time plot for the different loading cases.

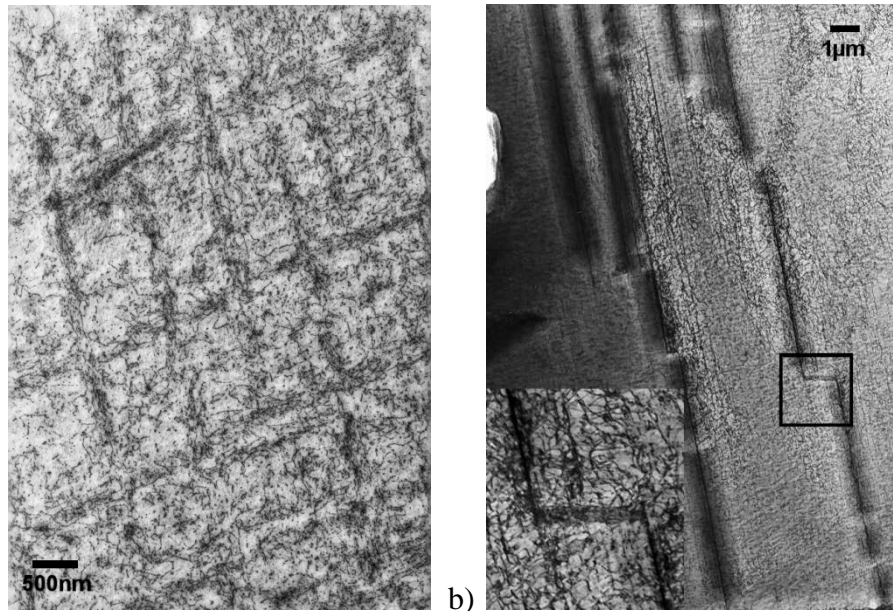


Figure 6: TEM micrographs for specimen after pure torsion loading with 0.5% equivalent strain, $N_f/2=13,500$ cycles, a) area with persistent lüders bands (PLBs), b) area with additional strain localization.

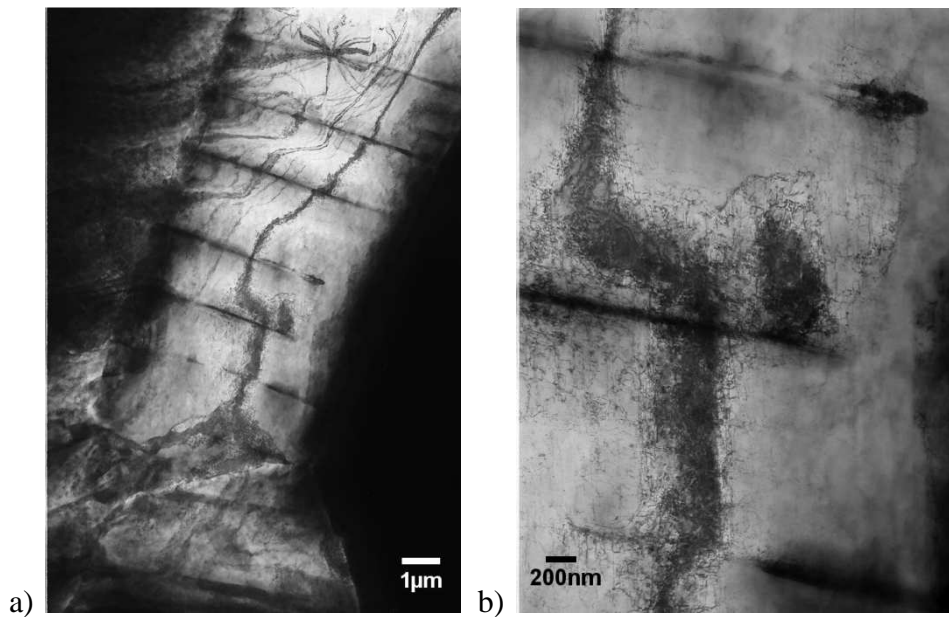


Figure 7: TEM micrographs for specimen after out of phase tension-torsion loading with circle path and 0.5% equivalent strain at $N_f/2=600$ cycles showing areas with pronounced strain localization: a) general view with bending contour from preparation, b) enlarged picture.



Figure 8: Inverted ECCI micrograph for a specimen with tension-torsion deformation on the circle path and 1% equivalent strain at $N_f=45$ cycles showing area with additional strain localization (micro twins).

SUMMARY AND CONCLUSIONS

Total strain controlled LCF experiments were carried out on α -brass CuZn30 in uniaxial tension-compression, pure torsion, planar biaxial and tension-torsion loading. The stress amplitudes under uniaxial and biaxial in phase loading conditions using the maximum

shear strain energy criterion are in good agreement. Pure torsion loading results in the highest stress amplitudes for all synchronous cases. The out of phase tests exhibit shorter life times and higher stress responses, especially under the tension-torsion loading conditions. The estimation of the non proportional hardening factor from uniaxial stress strain curves according to Shamsaei and Fatemi [6] results in a conservative approximation. The highest damage and hardening was observed in the circle path. The microstructure showed always planar dislocation structures. Dislocation arrangements according to wavy glide behavior were not observed. The proportional cases showed intense shear bands. These bands were not found in the non proportional tension-torsion test. In the samples with torsional loading additional locations were found which might be micro twins.

ACKNOWLEDGEMENT

Many thanks go to Dr. H.-A. Kuhn, Wieland-Werke AG for providing the test material.

REFERENCES

1. Doong, S.; Socie, D. & Robertson, I. (1990), Dislocation substructures and nonproportional hardening, *Journal of Engineering Materials and Technology* **112**, 456-464.
2. Zhang, J. & Jiang, Y. (2005), An experimental investigation on cyclic plastic deformation and substructures of polycrystalline copper, *International Journal of Plasticity* **21**, 2191-2211.
3. Jiao, F.; Österle, W.; Portella, P.D. & Ziebs, J. (1995), Biaxial path-dependence of low-cycle fatigue behaviour and microstructure of alloy 800 H at room temperature, *Materials Science and Engineering A* **196**, 19–24.
4. Reinhard, L.; Schönfeld, B.; Kostorz, G. & Bührer, W. (1990), Short-range order in α -brass, *Physical Review B* **41**, 1727–1734.
5. Kulawinski, D.; Nagel, K.; Henkel, S.; Hübner, P.; Fischer, H.; Kuna, M.; Biermann, H. (2011) Characterization of stress–strain behavior of a cast TRIP steel under different biaxial planar load ratios, *Engineering Fracture Mechanics* **78**, 1684-1695
6. Shamsaei, N. and Fatemi, A. (2010), Effect of microstructure and hardness on non-proportional cyclic hardening coefficient and predictions, *Materials Science and Engineering A* **527**, 3015–3024.
7. Laird, C. and Buchinger, L. (1985) *Hardening behavior in fatigue*, *Metallurgical and Materials Transactions A* **16**, 2201–2214
8. Carstensen, J. (1998) *Structural evolution and mechanisms of fatigue in polycrystalline brass*. Ph.D. thesis Risø-R-1005(EN), Risø National Laboratory, Denmark